Sulforaphane Inhibits Prostate Carcinogenesis and Pulmonary Metastasis in TRAMP Mice in Association with Increased Cytotoxicity of Natural Killer Cells

Shivendra V. Singh,[1,2] Renaud Warin,[1] Dong Xiao,[1] Anna A. Powolny,[1] Silvia D. Stan,[1] Julie A. Arlotti,[2] Yan Zeng,[2] Eun-Ryeong Hahm,[1] Stanley W. Marynowski,[2] Ajay Bommareddy,[1] Dhimant Desai,[4] Shantu Amin,[4] Robert A. Parise,[2,3] Jan H. Beumer,[2,3] and William H. Chambers[2]

[1]Department of Pharmacology and Chemical Biology, [2]University of Pittsburgh Cancer Institute, University of Pittsburgh School of Medicine; [3]Department of Pharmaceutical Sciences, University of Pittsburgh School of Pharmacy, Pittsburgh, Pennsylvania and [4]Department of Pharmacology, Penn State Milton S. Hershey Medical Center, Hershey, Pennsylvania

Abstract

The present study shows that oral gavage of 6 μmol D,L-sulforaphane (SFN), a synthetic analogue of cruciferous vegetable-derived L isomer, thrice per week beginning at 6 weeks of age, significantly inhibits prostate carcinogenesis and pulmonary metastasis in TRAMP mice without causing any side effects. The incidence of the prostatic intraepithelial neoplasia and well-differentiated (WD) carcinoma were ~23% to 28% lower ($P < 0.05$ compared with control by Mann-Whitney test) in the dorsolateral prostate (DLP) of SFN-treated mice compared with controls, which was not due to the suppression of T-antigen expression. The area occupied by the WD carcinoma was also ~44% lower in the DLP of SFN-treated mice relative to that of control mice ($P = 0.0011$ by Mann Whitney test). Strikingly, the SFN-treated mice exhibited ~50% and 63% decrease, respectively, in pulmonary metastasis incidence and multiplicity compared with control mice ($P < 0.05$ by t test). The DLP from SFN-treated mice showed decreased cellular proliferation and increased apoptosis when compared with that from control mice. Additionally, SFN administration enhanced cytotoxicity of cocultures of natural killer (NK) cells and dendritic cells (DC) against TRAMP-C1 target cells, which correlated with infiltration of T cells in the neoplastic lesions and increased levels of interleukin-12 production by the DC. In conclusion, the results of the present study indicate that SFN administration inhibits prostate cancer progression and pulmonary metastasis in TRAMP mice by reducing cell proliferation and augmenting NK cell lytic activity. [Cancer Res 2009;69(5):2117–25]

Introduction

Epidemiologic studies continue to support the premise that dietary intake of cruciferous vegetables may be protective against different types of malignancies, including prostate cancer (1–3). The anticarcinogenic effect of cruciferous vegetables is attributed to organic isothiocyanates (ITC), which are generated via myrosinase-mediated hydrolysis of corresponding glucosinolates (4, 5). The ITC compound (−)-1-isothiocyanato-(4*R*)-(methylsulfinyl)-butane (L-SFN) and its synthetic analogue D,L-sulforaphane (SFN) have generated a great deal of research interest because of their remarkable anticancer effects (4–7). For example, L-SFN and SFN are equipotent inducers of quinone reductase in Hepa1c1c7 murine hepatoma cells (6). The L-SFN or SFN administration has been shown to offer protection against 9,10-dimethyl-1,2-benzanthracene–induced mammary cancer in rats, azoxymethane-induced colonic aberrant crypt foci in rats, and benzo(*a*)pyrene–induced forestomach cancer in mice (8–10). Dietary feeding of SFN and its *N*-acetylcysteine conjugate inhibited malignant progression of lung adenomas induced by tobacco carcinogens in A/J mice (11).

Recent studies, including those from our laboratory, have documented novel cellular responses to SFN treatment in cultured human cancer cells, including growth arrest, induction of apoptosis and autophagy, inhibition of histone deacetylase, binding to proteins, and sensitization of cells to TRAIL-induced apoptosis (12–21). The mechanism by which SFN causes growth arrest and apoptosis induction has been extensively studied in human prostate cancer cells (13, 14, 16–18, 22). For example, we have shown previously that exposure of human prostate cancer cells to SFN results in G_2-M phase cell cycle arrest via checkpoint kinase 2–mediated phosphorylation of cell division cycle 25C (13). We also showed that the SFN-induced apoptosis was selective toward prostate cancer cells and linked to generation of reactive oxygen species (15, 16). Moreover, oral gavage of SFN in male nude mice significantly retarded the growth of PC-3 human prostate cancer xenografts *in vivo* (22).

Demonstration of *in vivo* efficacy of potential cancer chemopreventive agents in suitable animal models is a prerequisite for their further clinical development. The present study was designed to test whether SFN administration offers protection against prostate carcinogenesis in a transgenic mouse model of prostate cancer, TRAMP (transgenic adenocarcinoma of mouse prostate). We now show that oral gavage of SFN significantly prevents prostate cancer progression and pulmonary metastasis in TRAMP mice without causing any side effects or affecting the T-antigen expression.

Materials and Methods

Synthesis of SFN. SFN was synthesized as described by Conaway and colleagues (11). The structure of SFN was confirmed by proton nuclear magnetic resonance and mass spectrometry. The purity of the SFN (>99% pure) preparation was determined by high-performance liquid chromatography (HPLC), as described by Conaway and colleagues (11). SFN was stored at −20°C and found to be stable for at least 6 mo.

Cell viability and apoptosis assays. Monolayer cultures of TRAMP-C1 cells, a generous gift from Dr. Barbara Foster (Roswell Park Cancer

Requests for reprints: Shivendra V. Singh, 2.32A Hillman Cancer Center Research Pavilion, 5117 Center Avenue, Pittsburgh, PA 15213. Phone: 412-623-3263; Fax: 412-623-7828; E-mail: singhs@upmc.edu.

doi:10.1158/0008-5472.CAN-08-3502

Institute), were maintained in DMEM supplemented with 10% heat-inactivated fetal bovine serum, 10^{-8} mol/L 5α-androstan-17β-ol-3-one, and antibiotics in a humidified atmosphere of 95% air and 5% CO_2. Stock solution of SFN was prepared in DMSO, and an equal volume of DMSO (final concentration, <0.1%) was added to controls. Effect of SFN treatment on TRAMP-C1 cell viability was determined by trypan blue dye exclusion assay, as described by us previously (23). The proapoptotic effect of SFN was assessed by the analysis of cytoplasmic histone-associated DNA fragmentation and subdiploid cells, as described by us previously (23, 24).

Immunoblotting. The control and SFN-treated cells were lysed, as described by us previously (25). Prostate/tumor tissues were thawed on ice, and samples weighing ~100 mg were minced and homogenized in 5 volumes of ice-cold PBS containing protease and phosphatase inhibitors. Tissue homogenates were centrifuged at 5,000 × *g* for 10 min at 4°C to remove tissue debris followed by centrifugation at 14,000 × *g* for 30 min to obtain clear supernatants. Immunoblotting was performed as described by us previously (23–25).

SFN treatment. We selected TRAMP mice for the studies described herein because (*a*) a well-defined course of disease progression with similarities to human prostate carcinogenesis from histologic prostatic intraepithelial neoplasia (PIN) to well-differentiated (WD) and poorly differentiated (PD) carcinoma and distant site metastasis renders TRAMP mice suitable for chemoprevention studies (26–28), (*b*) the chemoprevention studies in TRAMP mice can be completed in a reasonable time frame (27, 28), and (*c*) the TRAMP model has been used successfully to test chemopreventive efficacy of several natural agents (29–32). Male TRAMP[C57BL/6xFVB]F1 hybrid mice were generated by breeding female TRAMP on a C57BL/6 background with nontransgenic FVB male mice. Male TRAMP mice were identified by PCR using DNA obtained from tail clippings (27). After transgene verification, male TRAMP mice were maintained in a climate-controlled environment with a 12-h light/12-h dark cycle and fed food and water *ad libitum*. At 6 to 7 wk of age, mice were randomized into two groups. Mice in the control group (n = 14) received 0.1 mL PBS by oral gavage thrice per week (Monday, Wednesday, and Friday), whereas the experimental mice (n = 13) received 6 μmol SFN in 0.1 mL PBS by oral gavage thrice per week for 17 to 19 wk. Body weights of the control and SFN-treated mice were recorded once each week beginning at the onset of the study. The mice were sacrificed 24 h after the last administration of the vehicle or SFN by CO_2 inhalation. A portion of the prostate/tumor tissue was placed in 10% neutral buffered formalin and paraffin-embedded.

Pathologic evaluation and scoring of tumor stage. Ten randomly selected fields of H&E-stained sections of the dorsolateral prostate (DLP) from individual mice of both control and SFN-treated groups were independently scored by two researchers for incidence and percentage of area corresponding to each pathologic stage. Pathologic grading was performed according to the recommendations of Greenberg and colleagues (27, 28), as described by us previously (32). Lung and pelvic lymph nodes were evaluated for the presence of metastasis by two independent researchers.

Pharmacokinetic study. Groups of male nontransgenic mice (n = 3, 6–8 wk of age) were gavaged with 6 μmol SFN in 0.1 mL PBS. Mice were sacrificed at specified time intervals, and plasma and lung tissue were collected and kept frozen at −80°C. Plasma (0.1 mL) or a 1:3 (w/v) homogenate of lung tissue in PBS (0.2 mL) was mixed with 10 μL of

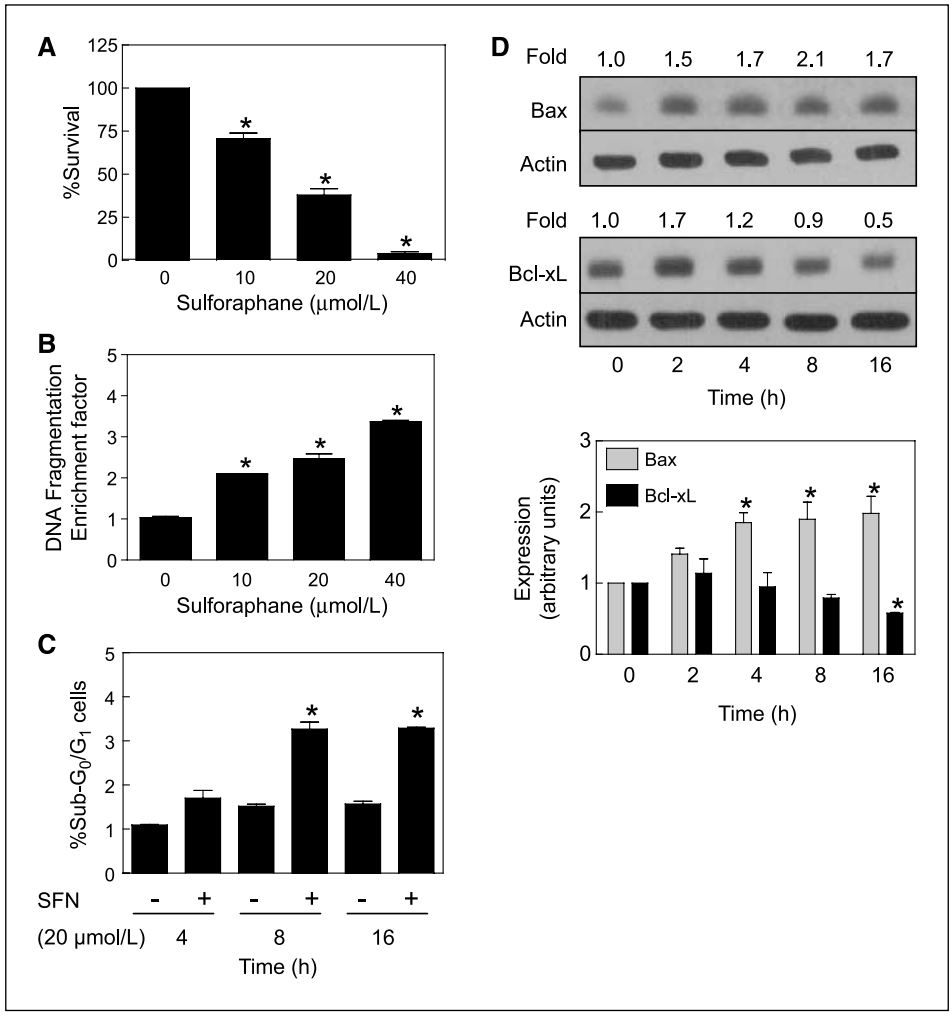

Figure 1. *A,* effect of SFN (24-h treatment) on viability of TRAMP-C1 cells. *B,* cytoplasmic histone-associated DNA fragmentation in TRAMP-C1 cells resulting from a 24-h exposure to DMSO or SFN. *C,* percentage of subdiploid apoptotic cells in TRAMP-C1 treated with DMSO or 20 μmol/L SFN for the indicated time periods. *D,* immunoblotting for Bax and Bcl-xL using lysates from TRAMP-C1 cells treated with 20 μmol/L SFN for the indicated time periods. Densitometric scanning data after correction for actin loading control are shown on top of the bands. *Columns,* mean (*A–C,* n = 3; *D,* n = 2); *bars,* SE. *, significantly different (P < 0.05) compared with control by one-way ANOVA followed by Dunnett's test.

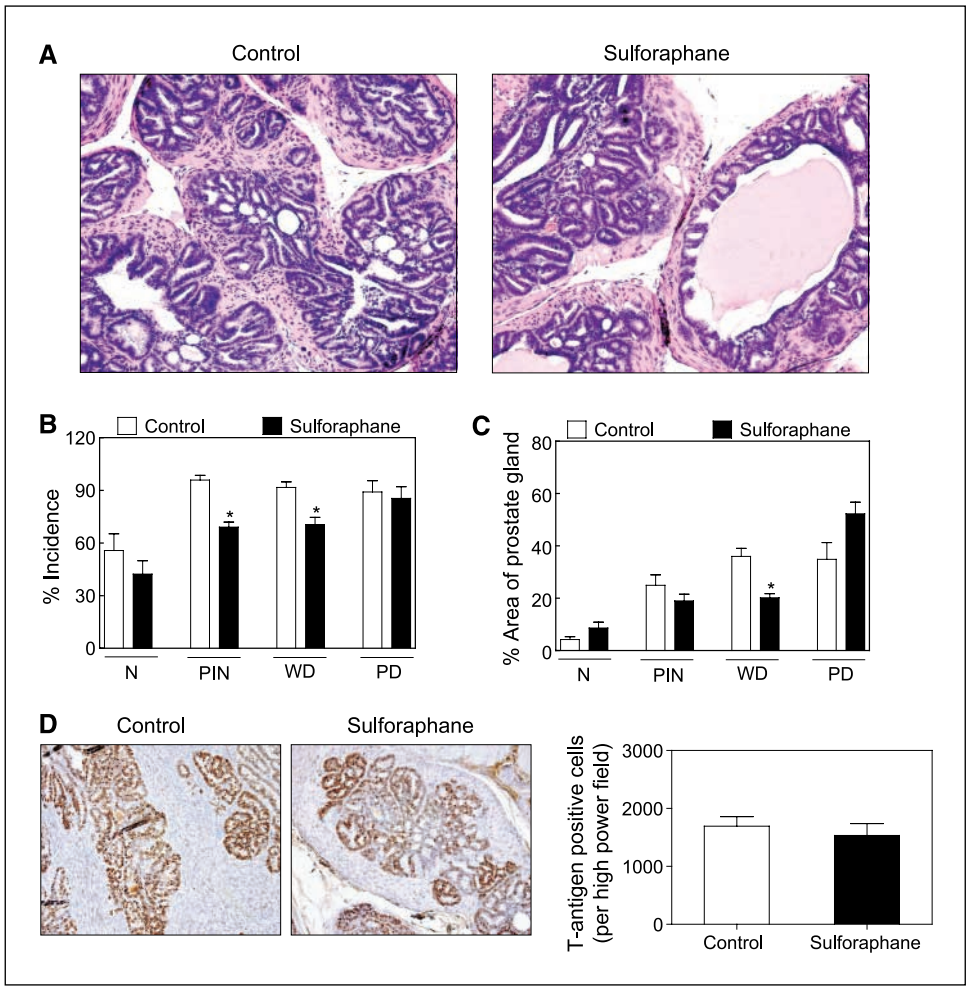

Figure 2. *A,* H&E staining in the DLP from representative mouse of both vehicle-treated control and SFN treatment groups (magnification, 200×). *B,* incidence of histologic grades classified as normal prostate (*N*), PIN, WD carcinoma, and PD carcinoma in the DLP from vehicle-treated control mice and SFN-treated mice. Ten representative fields of each section were scored for incidence of each histologic grade. The error bars represent variability of results in histologic grading between the two researchers. *C,* percentage of the area corresponding to the normal prostate, PIN, WD carcinoma, and PD carcinoma in the DLP of control and SFN-treated mice. The scores of the two researchers were averaged and expressed as mean ± SE. *B* and *C,* *, significantly different compared with control by Mann-Whitney test. *D,* T-antigen expression in representative DLP of a control and an SFN-treated TRAMP mouse (magnification, 200×). The bar graph represents quantitative analysis of T-antigen expression. *Columns,* mean (n = 4); *bars,* SE.

10 μg/mL alyssin (internal standard, LKT Laboratories). Lung homogenates were mixed with 1 mL of acetonitrile and centrifuged at 16,000 × g for 5 min at room temperature. The resulting supernatants were evaporated to dryness under a gentle stream of nitrogen at 37°C and reconstituted in 200 μL distilled water/formic acid (200:10, v/v). Plasma samples were mixed with 5 μL formic acid. Each reconstituted lung or plasma sample was applied to a Bond Elute (C2, 500 mg, 3 mL) solid-phase cartridge (Varian) preconditioned with 2 mL of methanol and 2 mL of 1% formic acid. The cartridges were washed with 2 mL of distilled water/methanol (95:5, v/v). The SFN and the internal standard were eluted with 2 mL of acetonitrile, and the eluates were evaporated to dryness under a gentle stream of nitrogen at 37°C. Each dried residue was reconstituted in 100 μL of acetonitrile/distilled water (15:85, v/v) and transferred to an autosampler vial, and 10 μL were injected into the HPLC system. The HPLC system consisted of an Agilent model 1100 autosampler and binary pump (Agilent Technologies) and a Phenomenex Hydro-Synergi RP (4 μm, 100 × 2 mm) reverse-phase analytic column. A gradient mobile phase consisting of solvent A (acetonitrile/formic acid, 99.9%/0.1%) and solvent B (water/formic acid, 99.9%/0.1%) was used for separation. The initial condition was 15% solvent A (2 min), which increased linearly in 8 min to 40% solvent A. This condition was held for 5 min, and then solvent A was linearly returned to 15% at 16 min. This condition was held for 8 min. The flow rate was 0.2 mL/min. The SFN and the internal standard were detected using a ThermoFinnigan MSQ Mass Spectrometer (Thermo Electron) operating in positive electrospray, single-ion mode monitoring m/z 177.7 for SFN and m/z 191.7 for alyssin. Concentrations of SFN were determined by calculating the ratio of SFN peak area to that of the internal standard and back-calculating the concentration of SFN in the unknown samples with a concomitantly analyzed standard curve in the respective matrix. Standard curves were linear over the range of 10 to 10,000 ng/mL and displayed acceptable performance (accuracy within 15% of nominal concentrations and precision <15% at all concentrations). Pharmacokinetic data were analyzed noncompartmentally with PK Solutions 2.0 (Summit Research Service[5]).

Immunohistochemical analyses of T-antigen, proliferating cell nuclear antigen, CD31, and E-cadherin expression and quantitation of apoptotic bodies. Tissues were sectioned at 4 to 5 μm thickness, deparaffinized, and rehydrated. Immunohistochemical analysis of T-antigen, proliferating cell nuclear antigen (PCNA), CD31, and E-cadherin expression was performed, as described by us previously (32). Apoptotic bodies were visualized by TUNEL staining, as described by us previously (32). The images were analyzed using Image ProPlus 5.0 software (Media Cybernetics) for quantitation of T-antigen, PCNA, and E-cadherin expression, as well as for analysis of microvessel number (CD31 staining).

Cytotoxicity of natural killer cells and dendritic cells. After transgene verification, male TRAMP mice (ages, 6–7 wk) were randomized into two groups with six mice per group. The mice were gavaged thrice weekly (Monday, Wednesday, and Friday) with either 6 μmol SFN in 0.1 mL PBS or vehicle (control) for 13 wk. We reasoned that SFN-mediated inhibition of prostate carcinogenesis in TRAMP mice may be preceded by augmentation of natural killer (NK)/dendritic cell (DC) function, which prompted us to terminate this experiment at an earlier time point. The mice were then sacrificed, and the spleen and bone marrow were harvested from mice of each group for isolation of NK cells and DCs, respectively, as described by us

[5] http://www.summitPK.com

previously (32). Cytotoxicity of NK and/or DC toward TRAMP-C1 target cells was determined using the Cytotox 96 nonradioactive assay, as described previously by us (32). Quantitation of T-cell and NK cell infiltration in the DLP was performed by immunohistochemical analysis of CD3+ and CD57+ cells, respectively, using the double-stain kit from Biocare Medical according to the manufacturer's protocol.

Quantitation of interleukin-12 and IFNγ release. Spleen-derived NK cells and bone marrow–derived DCs from control and SFN-treated mice were cultured for 5 d, and the culture media were then collected and analyzed for IFNγ and interleukin-12 (IL-12) release, respectively, using ELISA kits from Biosource.

Results

SFN treatment decreased viability of TRAMP-C1 cells by causing apoptosis. As can be seen in Fig. 1*A*, the viability of TRAMP-C1 cells was decreased significantly after a 24-hour exposure to SFN in a dose-dependent manner. The SFN-mediated suppression of TRAMP-C1 cell viability correlated with apoptosis induction, as revealed by a dose-dependent increase in cytoplasmic histone-associated DNA fragmentation (Fig. 1*B*) and enrichment of subdiploid apoptotic fraction (Fig. 1*C*). Moreover, consistent with the results in human prostate cancer cells (16, 22), SFN treatment caused induction of multidomain proapoptotic protein Bax and down-regulation of antiapoptotic Bcl-xL protein (Fig. 1*D*).

Oral administration of SFN inhibited prostate cancer progression in TRAMP mice. Next, we proceeded to determine the effect of SFN administration on prostate carcinogenesis using TRAMP mice. We have shown previously that thrice weekly oral gavage of 6 μmol SFN is highly effective in suppressing growth of PC-3 xenografts in male nude mice (22). We used a similar dosing regimen in the present study to determine efficacy of SFN against prostate carcinogenesis in TRAMP mice. Representative H&E staining in sections of DLP from control and SFN-treated mice are depicted in Fig. 2*A*. The DLP of the vehicle-treated control TRAMP mice exhibited low-grade and high-grade PIN and WD and PD carcinomas along with areas consistent with normal prostate. The

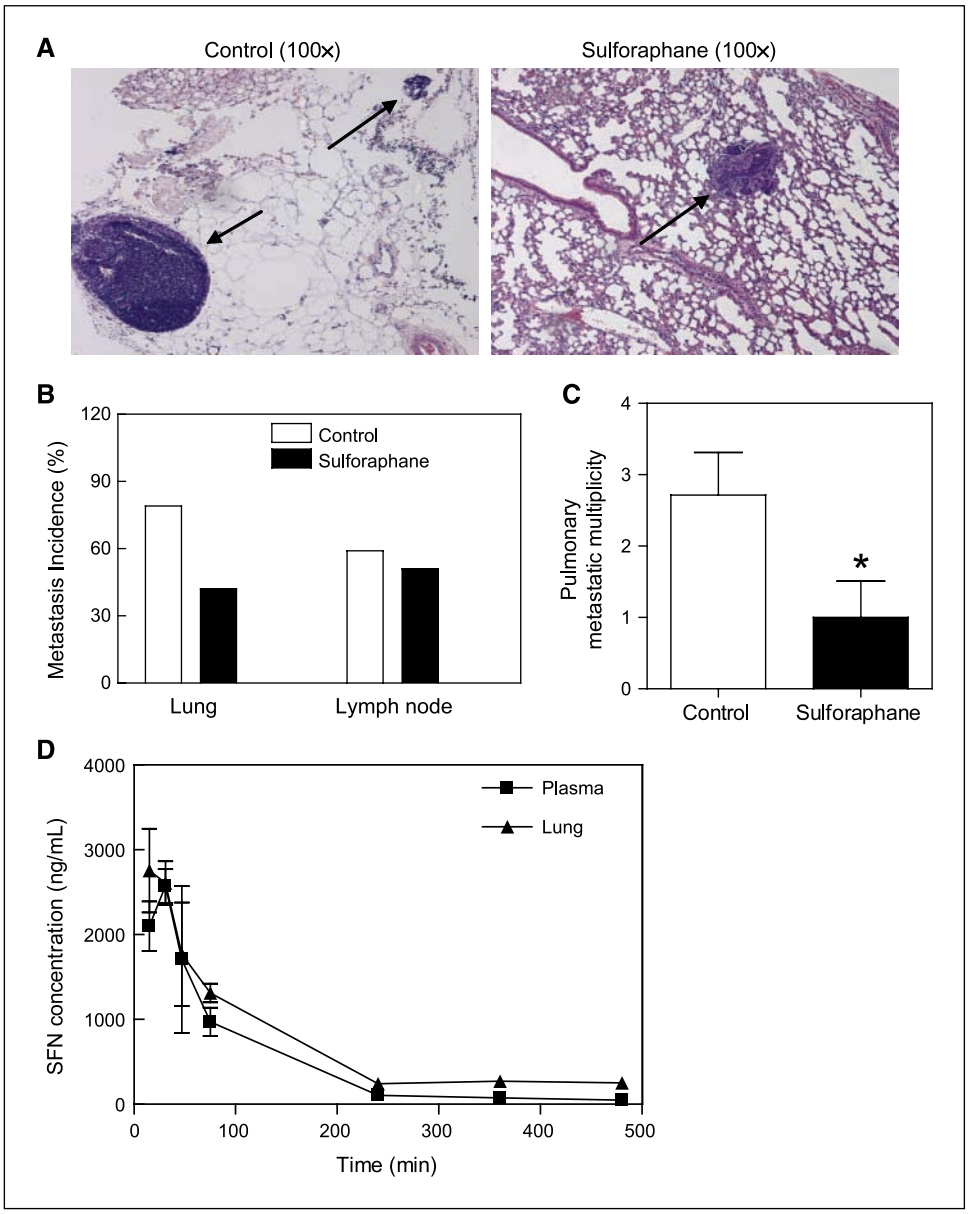

Figure 3. *A,* representative H&E stain showing metastatic lesions (*arrows*) in the lungs of control and SFN-treated mice. Incidence of metastasis (*B*) and pulmonary metastasis multiplicity (*C*) in control and SFN-treated mice. *Columns,* mean (n = 12–14); *bars,* SE. *, significantly different (P < 0.05) compared with the vehicle-treated control group by t test. *D,* plasma and lung concentrations of SFN versus time after oral gavage of male nontransgenic mice with 6 μmol SFN. *Points,* mean (n = 3); *bars,* SE. Data for lung represents ng SFN/g tissue.

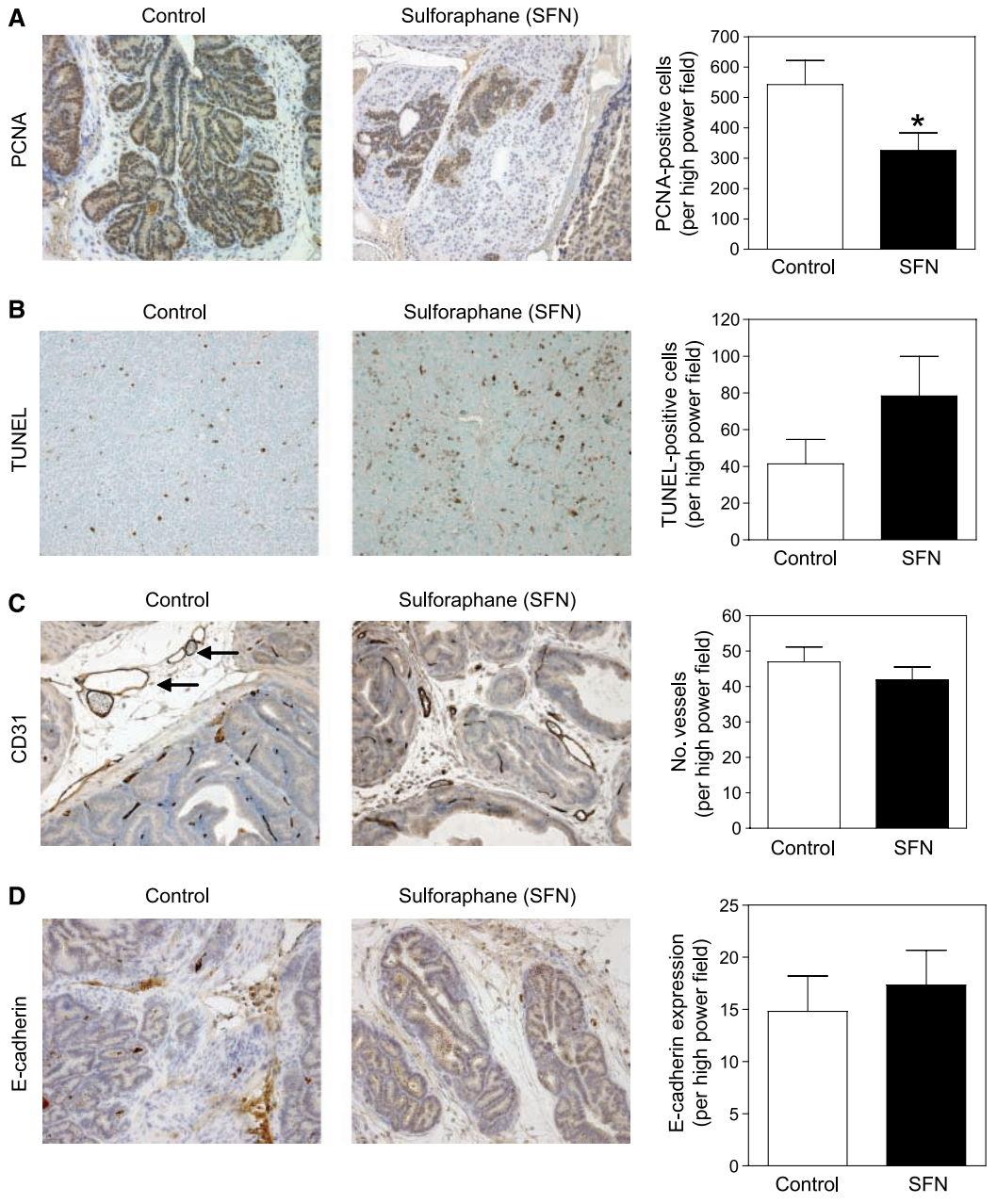

Figure 4. Analyses for expression of PCNA (*A*), TUNEL-positive apoptotic bodies (*B*), CD31 (*C*) to visualize blood vessels (*arrows*), and E-cadherin expression (*D*) in the DLP of a representative mouse of both the control and SFN treatment groups (magnification, 200×). *Right,* quantitative results for each variable. *Columns,* mean (n = 6–7); *bars,* SE. *, significantly different ($P < 0.05$) compared with control by t test.

incidence of the PIN and WD carcinoma in the DLP of mice treated with SFN was lower by 28% (P = 0.006 by Mann-Whitney test) and 23% (P = 0.0104), respectively, in comparison with control mice (Fig. 2*B*). The area occupied by the WD in the DLP of SFN-treated mice was lower by ~44% (P = 0.0011 by Mann-Whitney test) compared with control mice (Fig. 2*C*). Although the area occupied by the PIN in the DLP of SFN-treated mice was lower by ~24% compared with control, the difference did not reach statistical significance. The body weights of the control and SFN-treated mice did not differ significantly throughout the experimental protocol (results not shown). The mice of both groups were monitored on alternate days for signs of stress throughout the experimental protocol. Except for some mice that were moribund due to large tumor burden before the termination of the experiment, control and SFN-treated mice did not exhibit signs of stress, including food and water withdrawal, impaired posture or movement, ruffled fur, areas of redness or swelling, and indigestion. Moreover, the vital organs (liver, kidney, lung, and heart) from control and SFN-treated mice were histologically normal, except for microscopic evidence of pulmonary metastasis. However, the SFN-mediated inhibition of prostate carcinogenesis was not due to suppression of T-antigen expression (Fig. 2*D*).

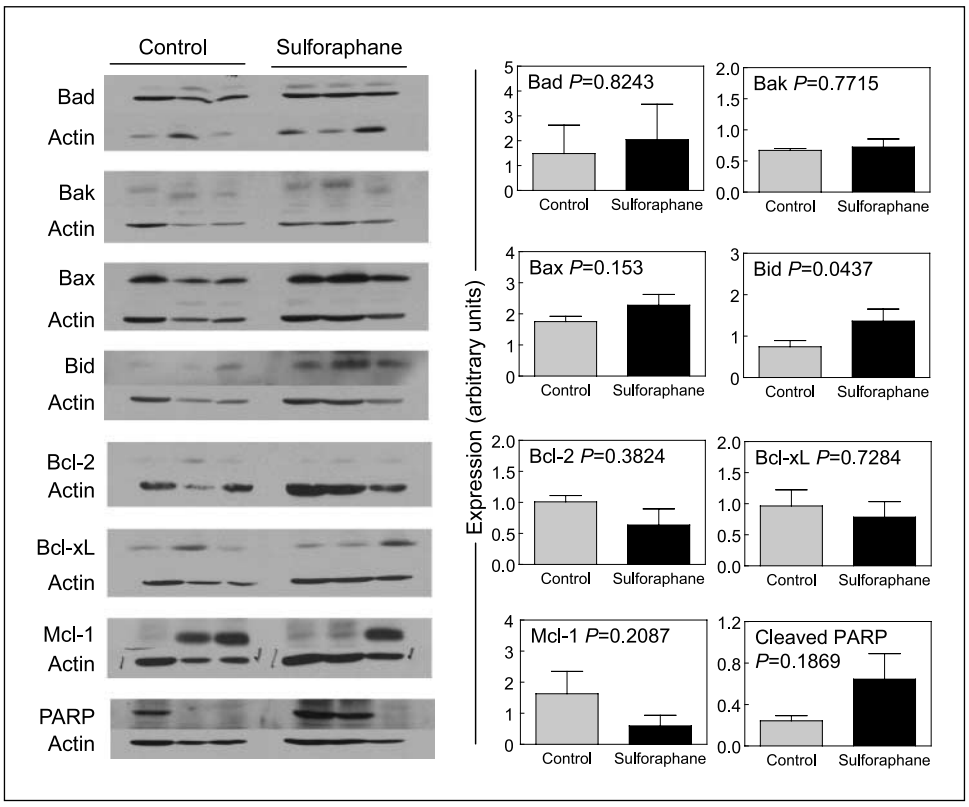

Figure 5. Immunoblotting for Bcl-2 family proteins and cleaved PARP using prostate/tumor supernatants from three different mice of both control and SFN-treated groups. The blots were stripped and reprobed with antiactin antibody to normalize for differences in protein loading. *Right,* quantitative results for each protein. *Columns,* mean (n = 3); *bars,* SE.

SFN administration inhibited pulmonary metastasis. Figure 3*A* depicts H&E staining in lung section of a representative mouse of both the control and SFN treatment group. The incidence of pulmonary metastasis was ~80% in vehicle-treated control mice, which was reduced to ~40% in the SFN treatment group (Fig. 3*B*). The incidence of metastasis to pelvic lymph nodes was comparable in control and SFN-treated mice (Fig. 3*B*). Multiplicity of pulmonary metastatic lesions in mice treated with SFN was lower by ~63% (P = 0.042 by t test) compared with control mice (Fig. 3*C*).

Pharmacokinetic measurements. We found that SFN was absorbed rapidly and reached a peak plasma concentration (C_{max}) of 3,410 ng/mL at a T_{max} of ~42 minutes (Fig. 3*D*). The terminal elimination half-life of SFN in plasma was ~255 minutes. The C_{max} of SFN in the lung was ~3,686 ng/g with a T_{max} of ~15 minutes. The area under the concentration versus time curve between 0 and 8 hours (AUC_{0-8}) of SFN in lung (5.80 μg/g·h) was 47% higher than the AUC_{0-8} of SFN in plasma (3.94 μg/mL·h).

SFN administration decreased cell proliferation. We determined expression of PCNA, a well-accepted marker of cell proliferation (33), by immunohistochemistry to test whether SFN-mediated suppression of prostate carcinogenesis was due to inhibition of cellular proliferation. As can be seen in Fig. 4*A*, PCNA expression was ~40% lower in the DLP of mice treated with SFN compared with control mice (P = 0.028 by t test). The fraction of TUNEL-positive apoptotic bodies was ~1.9-fold higher in the DLP of SFN-treated mice compared with the controls, but the difference was statistically insignificant due to large data scatter, especially in the SFN treatment group (Fig. 4*B*).

SFN exhibits antiangiogenic activity *in vitro* and *in vivo* (34). To test whether SFN administration caused suppression of neovascularization *in vivo*, the DLP from vehicle-treated control mice and SFN-treated mice were stained for angiogenic marker CD31. Immunohistochemical staining for CD31 in the DLP of representative mouse from both the control and SFN groups are shown in Fig. 4*C* (vessels are identified by arrows). The average number of vessels in the DLP did not differ significantly between control and SFN-treated mice (Fig. 4*C*).

E-cadherin is considered a suppressor of invasion and growth of many epithelial cancers (35). We, therefore, compared expression of E-cadherin in the DLP of control and SFN-treated mice. Expression of E-cadherin was slightly higher in the DLP of SFN-treated mice compared with that of control mice, but the difference was statistically insignificant. These results indicated that the SFN-mediated inhibition of prostate carcinogenesis correlated with decreased cellular proliferation, as well as a modest increase in the number of apoptotic bodies in the DLP.

Effect of SFN administration on levels of Bcl-2 family proteins. We compared expression of Bcl-2 family proteins using prostate/tumor supernatants to determine the mechanism of SFN-mediated apoptosis. As can be seen in Fig. 5, the levels of proapoptotic Bcl-2 family proteins Bad, Bak, Bax, and Bid were higher by ~1.33-fold, 1.16-fold, 1.27-fold, and 1.9-fold, respectively, in the prostate of SFN-treated mice compared with controls. Additionally, SFN administration resulted in a marked decrease (~63% decrease compared with control) in the level of antiapoptotic protein Mcl-1 compared with control (Fig. 5). The level of cleaved poly(ADP-ribose) polymerase (PARP) was ~2.7-fold higher in the prostate of SFN-treated mice compared with the control (Fig. 5).

SFN augmented cytotoxic activity of NK/DC cocultures against TRAMP-C1 cells. The NK cells play an important role in immunosurveillance during tumorigenesis (36, 37). The NK cells mediate cytotoxicity against tumor cells by multiple mechanisms, including granule-mediated exocytosis and induction of apoptosis (36). To assess if SFN administration affected NK cell/DC function,

we determined the cytotoxicity of NK cells and/or DC isolated from control and SFN-treated mice toward TRAMP-C1 as a target cell line. The results in Fig. 6*A* show that the NK cells isolated from the spleen of SFN-treated TRAMP mice were more cytotoxic against TRAMP-C1 cells compared with the NK cells isolated from control mice (23% versus 50% cytotoxicity for NK cells isolated from control and SFN-treated mice, respectively; $P < 0.05$ by t test). It is well established that interactions of NK cells with DC result in coactivation of both cell types (38). We, therefore, determined the lytic functions of NK cell and DC cocultures. The cytotoxic activity of NK cells against TRAMP-C1 cells was increased even more with coculture of NK cells with DC at 10:8 ratio compared with NK cells alone. This effect correlated with a significant increase in IL-12 production by the DC isolated from the bone marrow of SFN-treated mice compared with control mice (Fig. 6*B, left*). On the other hand, the IFNγ production by the NK cells did not differ significantly between control and SFN-treated mice (Fig. 6*B, right*). Altogether, these results indicate that SFN administration stimulates immune response by augmenting NK cell lytic function through DC-mediated IL-12 production.

SFN administration caused T-cell infiltration in the prostate tumor. Next, we explored the possibility of whether the prostate tumor from SFN-treated mice was infiltrated by carriers of an adaptive immune response, such as T cells. We stained prostate

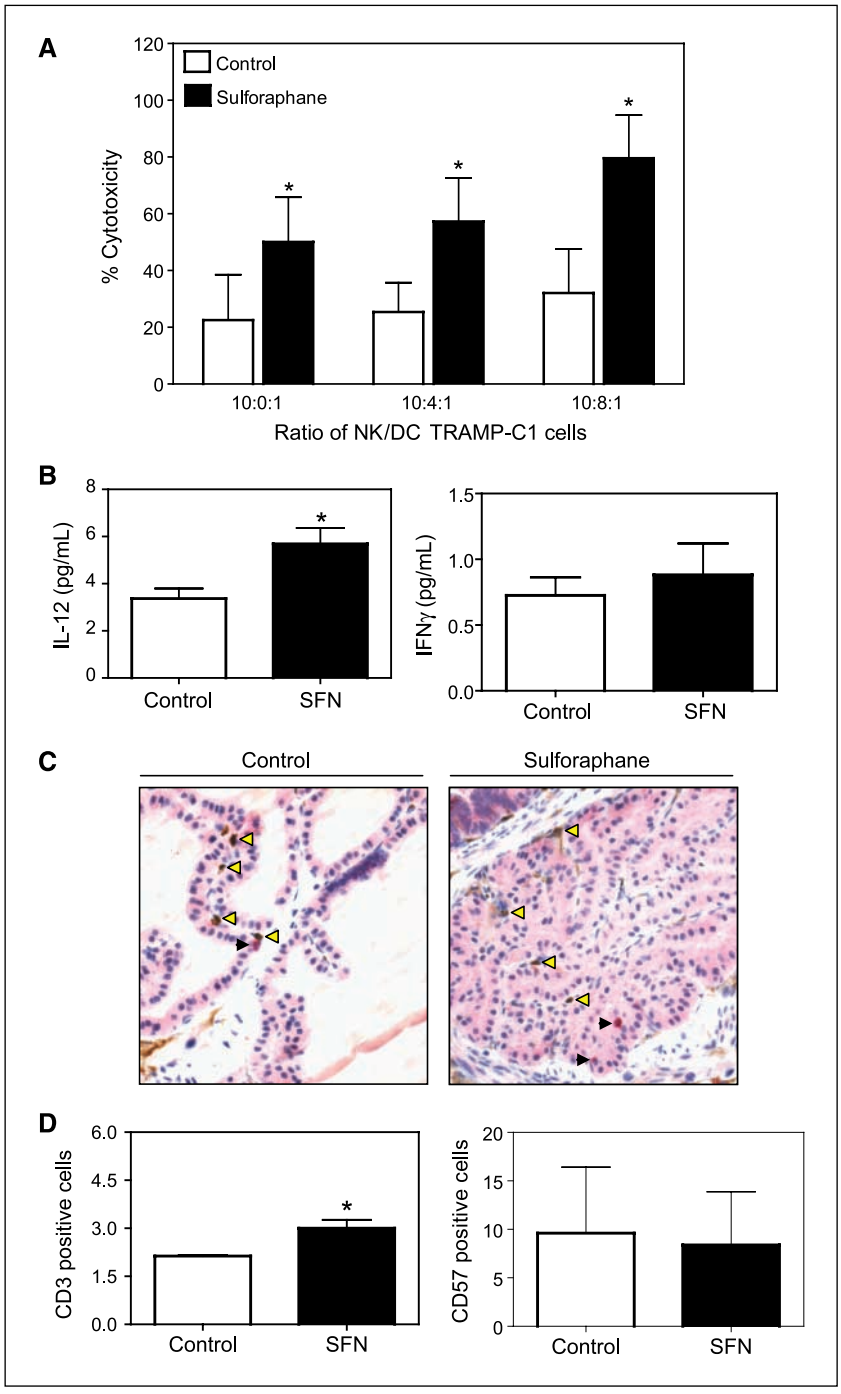

Figure 6. *A,* cytotoxicity of NK alone and NK/DC cocultures toward TRAMP-C1 target cells. The NK/DC were incubated together at the desired ratio for 24 h before the addition of TRAMP-C1 target cells. *B,* IL-12 (*left*) and IFNγ (*right*) levels in DC and NK culture medium after 5 d, respectively. *C,* immunohistochemical analysis for CD3-positive T-cell infiltration and CD57-positive NK cell infiltration in representative prostate of a control mouse and an SFN-treated mouse. The CD3-positive and CD57-positive cells are identified by yellow and black arrowheads, respectively (magnification, 400×). *D,* quantification of CD3+ T-cell and CD57+ NK cell infiltration in prostate tumor of control and SFN-treated animals. Ten representative fields of each section were evaluated and averaged for CD3+ and CD57+ cells. *Columns,* mean (*A–B,* $n = 6$; *D,* $n = 3$); *bars,* SE. *, significantly different ($P < 0.05$) compared with control by t test.

tumors from control and SFN-treated mice using anti-CD3 (a marker of T cells) and anti-CD57 (a marker of NK cells) antibodies. The results can be visualized in Fig. 6*C*, where NK cells are stained in brown and the T cells are stained in pink. The prostate tumors from SFN-treated mice exhibited a modest yet statistically significant increase in T-cell, but not NK cell, infiltration compared with control (Fig. 6*D*). Taken together, our results indicate that SFN administration increases immunosurveillance by boosting both the NK cell lytic function and T-cell infiltration.

Discussion

The present study shows that SFN not only suppresses the growth of a TRAMP tumor–derived cell line in culture but also prevents incidence and/or burden of PIN and well-differentiated carcinoma and incidence and multiplicity of lung metastasis in male TRAMP mice without causing weight loss or affecting the T-antigen expression. The possibility that higher concentration of SFN and/or a more intensive dosing regimen (e.g., daily administration) results in better chemopreventive response cannot be ruled out. Likewise, it is possible that earlier onset of SFN administration (e.g., starting at 4–5 weeks of age) leads to even greater protection against prostate carcinogenesis in TRAMP mice. Additional work is needed to systematically explore these possibilities.

The bioavailability of SFN in TRAMP mice is yet to be evaluated, but this variable has been determined in rats. The SFN was detectable in the plasma after 1 hour of oral gavage of rats with 50 μmol SFN (39). The maximal plasma concentration of SFN was found to be ~20 μmol/L after 4 hours of oral gavage and declined with a half-life of 2.2 hours (39). Hanlon and colleagues (40) have shown that SFN is rapidly absorbed with an absolute bioavailability of ~82% in rats (40). The maximal plasma concentration of SFN and its cysteine conjugate varied between 0.65 and 0.82 μmol/L in healthy human volunteers, who consumed a test meal of broccoli soup (150 mL) containing 100 g of broccoli (41). The SFN concentration effective against prostate carcinogenesis and pulmonary metastasis in TRAMP mice is well within the range that may not only be generated through dietary intake of cruciferous vegetables but can also be safely given to humans without any harmful side effects (5, 42).

We have shown previously that SFN treatment suppresses growth of cultured human prostate cancer cells by causing G_2-M phase cell cycle arrest and apoptosis induction (13, 16, 21, 22). The present study reveals that a cell line derived from the prostate tumor of a TRAMP mouse is also highly sensitive to growth inhibition and apoptosis induction by SFN treatment. We also found that oral administration of SFN causes a statistically significant decrease in cell proliferation in the DLP of TRAMP mice, as evidenced by reduced expression of PCNA. Moreover, the average number of TUNEL-positive apoptotic bodies was markedly higher in the DLP of SFN-treated mice in comparison with controls. Thus, it is reasonable to conclude that SFN-mediated inhibition of prostate carcinogenesis in TRAMP mice *in vivo* is mediated by reduced cellular proliferation and increased apoptosis.

Distant site metastasis is a major cause of death in prostate cancer patients (43). The pathogenesis of metastasis is complex and involves a series of molecular events, including synthesis and secretion of angiogenic factors to promote neovascularization, motility, and local invasion of the host stroma, entry into the circulation, detachment, and extravasation (44). Steps leading to metastasis are complex and regulated by multiple molecules, including growth factors, matrix metalloproteinases, and cell adhesion molecules (44). For example, loss of expression of cell adhesion molecules, especially E-cadherin, is believed to be important for development of metastatic lesions (35). Inhibition of prostate carcinogenesis and metastasis by the plant flavonoid apigenin in TRAMP mice was shown to correlate with retained expression of E-cadherin (29). The present study reveals that the SFN administration inhibits pulmonary metastasis incidence and multiplicity in TRAMP mice. However, the inhibitory effect of SFN administration against pulmonary metastasis seems independent of changes in E-cadherin expression or inhibition of angiogenesis. Delineation of the precise mechanisms by which SFN administration inhibits pulmonary metastasis awaits further work.

The present study shows, for the first time, that treatment of TRAMP mice with SFN leads to increased production of IL-12 by DC. This effect results in augmentation of NK cell cytotoxicity toward a prostate cancer cell line and increased efficiency of DC activation of NK cell cytotoxic function after their coculture. Previous studies have documented the capacity for DC to internalize, process and present tumor cell-derived antigens, and thereby to stimulate the antitumor function of both CTLs and IFNγ-producing NK cells (45, 46). In addition to the stimulatory effects of SFN administration on *in vitro* functions of NK cells and DC, we observed an increase in T-cell infiltration in the prostate tumors of SFN-treated TRAMP mice in comparison with control mice. Taken together, our results suggest that SFN can enhance immune function toward prostate tumors by stimulating IL-12 release by DC, leading to an increased level of cytotoxicity of NK cells and ultimately to a greater infiltration of prostate tumors by T cells, which results in a lower tumor burden and less metastases.

In conclusion, the results of the present study indicate that oral administration of SFN significantly inhibits prostate carcinogenesis and pulmonary metastasis in TRAMP mice without causing any harmful side effects or reducing T-antigen expression.

Disclosure of Potential Conflicts of Interest

No potential conflicts of interest were disclosed.

Acknowledgments

Received 9/9/2008; revised 11/19/2008; accepted 12/1/2008; published OnlineFirst 02/17/2009.

Grant support: National Cancer Institute US PHS grants CA115498 and CA101753.

The costs of publication of this article were defrayed in part by the payment of page charges. This article must therefore be hereby marked *advertisement* in accordance with 18 U.S.C. Section 1734 solely to indicate this fact.

References

1. Verhoeven DT, Goldbohm RA, van Poppel G, Verhagen H, van den Brandt PA. Epidemiological studies on *Brassica* vegetables and cancer risk. Cancer Epidemiol Biomarkers Prev 1996;5:733–48.
2. Kolonel LN, Hankin JH, Whittemore AS, et al. Vegetables, fruits, legumes and prostate cancer: a multiethnic case-control study. Cancer Epidemiol Biomarkers Prev 2000;9:795–804.
3. Ambrosone CB, McCann SE, Freudenheim JL, Marshall JR, Zhang Y, Shields PG. Breast cancer risk in premenopausal women is inversely associated with consumption of broccoli, a source of isothiocyanates, but is not modified by GST genotype. J Nutr 2004;134:1134–8.
4. Hecht SS. Inhibition of carcinogenesis by isothiocyanates. Drug Metab Rev 2000;32:395–411.

5. Conaway CC, Yang YM, Chung FL. Isothiocyanates as cancer chemopreventive agents: their biological activities and metabolism in rodents and humans. Curr Drug Metab 2002;3:233–55.
6. Zhang Y, Talalay P, Cho CG, Posner GH. A major inducer of anticarcinogenic protective enzymes from broccoli: isolation and elucidation of structure. Proc Natl Acad Sci U S A 1992;89:2399–403.
7. Brooks JD, Paton VG, Vidanes G. Potent induction of phase 2 enzymes in human prostate cells by sulforaphane. Cancer Epidemiol Biomarkers Prev 2001;10: 949–54.
8. Zhang Y, Kensler TW, Cho CG, Posner GH, Talalay P. Anticarcinogenic activities of sulforaphane and structurally related synthetic norbornyl isothiocyanates. Proc Natl Acad Sci U S A 1994;91:3147–50.
9. Chung FL, Conaway CC, Rao CV, Reddy BS. Chemoprevention of colonic aberrant crypt foci in Fischer rats by sulforaphane and phenethyl isothiocyanate. Carcinogenesis 2000;21:2287–91.
10. Fahey JW, Haristoy X, Dolan PM, et al. Sulforaphane inhibits extracellular, intracellular, and antibiotic-resistant strains of *Helicobacter pylori* and prevents benzo[*a*]pyrene-induced stomach tumors. Proc Natl Acad Sci U S A 2002;99:7610–5.
11. Conaway CC, Wang CX, Pittman B, et al. Phenethyl isothiocyanate and sulforaphane and their *N*-acetylcysteine conjugates inhibit malignant progression of lung adenomas induced by tobacco carcinogens in A/J mice. Cancer Res 2005;65:8548–57.
12. Gamet-Payrastre L, Li P, Lumeau S, et al. Sulforaphane, a naturally occurring isothiocyanate, induces cell cycle arrest and apoptosis in HT29 human colon cancer cells. Cancer Res 2000;60:1426–33.
13. Singh SV, Herman-Antosiewicz A, Singh AV, et al. Sulforaphane-induced G_2-M phase cell cycle arrest involves checkpoint kinase 2 mediated phosphorylation of Cdc25C. J Biol Chem 2004;279:25813–22.
14. Myzak MC, Hardin K, Wang R, Dashwood RH, Ho E. Sulforaphane inhibits histone deacetylase activity in BPH-1, LNCaP and PC-3 prostate epithelial cells. Carcinogenesis 2006;27:811–9.
15. Choi S, Singh SV. Bax and Bak are required for apoptosis induction by sulforaphane, a cruciferous vegetable derived cancer chemopreventive agent. Cancer Res 2005;65:2035–43.
16. Singh SV, Srivastava SK, Choi S, et al. Sulforaphane-induced cell death in human prostate cancer cells is initiated by reactive oxygen species. J Biol Chem 2005; 280:19911–24.
17. Xu C, Shen G, Chen C, Gelinas C, Kong AN. Suppression of NF-κB and NF-κB-regulated gene expression by sulforaphane and PEITC through IκBα, IKK pathway in human prostate cancer PC-3 cells. Oncogene 2005;24:4486–95.
18. Herman-Antosiewicz A, Johnson DE, Singh SV. Sulforaphane causes autophagy to inhibit release of cytochrome *c* and apoptosis in human prostate cancer cells. Cancer Res 2006;66:5828–35.
19. Kim H, Kim EH, Eom YW, et al. Sulforaphane sensitizes tumor necrosis factor-related apoptosis-inducing ligand (TRAIL)-resistant hepatoma cells to TRAIL-induced apoptosis through reactive oxygen species-mediated up-regulation of DR5. Cancer Res 2006;66:1740–50.
20. Mi L, Wang X, Govind S, et al. The role of protein binding in induction of apoptosis by phenethyl isothiocyanate and sulforaphane in human non-small lung cancer cells. Cancer Res 2007;67:6409–16.
21. Choi S, Lew KL, Xiao H, et al. D,L-Sulforaphane-induced cell death in human prostate cancer cells is regulated by inhibitor of apoptosis family proteins and Apaf-1. Carcinogenesis 2007;28:151–62.
22. Singh AV, Xiao D, Lew KL, Dhir R, Singh SV. Sulforaphane induces caspase-mediated apoptosis in cultured PC-3 human prostate cancer cells and retards growth of PC-3 xenografts *in vivo*. Carcinogenesis 2004; 25:83–90.
23. Xiao D, Choi S, Johnson DE, et al. Diallyl trisulfide-induced apoptosis in human prostate cancer cells involves c-Jun N-terminal kinase and extracellular-signal regulated kinase-mediated phosphorylation of Bcl-2. Oncogene 2004;23:5594–606.
24. Herman-Antosiewicz A, Singh SV. Checkpoint kinase 1 regulates diallyl trisulfide-induced mitotic arrest in human prostate cancer cells. J Biol Chem 2005;280: 28519–28.
25. Xiao D, Srivastava SK, Lew KL, et al. Allyl isothiocyanate, a constituent of cruciferous vegetables, inhibits proliferation of human prostate cancer cells by causing G_2-M arrest and inducing apoptosis. Carcinogenesis 2003;24:891–7.
26. Klein RD. The use of genetically engineered mouse models of prostate cancer for nutrition and cancer chemoprevention research. Mutat Res 2005;576:111–9.
27. Greenberg NM, DeMayo F, Finegold MJ, et al. Prostate cancer in a transgenic mouse. Proc Natl Acad Sci U S A 1995;92:3439–43.
28. Kaplan-Lefko PJ, Chen TM, Ittmann MM, et al. Pathobiology of autochthonous prostate cancer in a pre-clinical transgenic mouse model. Prostate 2003;55:219–37.
29. Shukla S, MacLennan GT, Flask CA, et al. Blockade of β-catenin signaling by plant flavonoid apigenin suppresses prostate carcinogenesis in TRAMP mice. Cancer Res 2007;67:6925–35.
30. Raina K, Singh RP, Agarwal R, Agarwal C. Oral grape seed extract inhibits prostate tumor growth and progression in TRAMP mice. Cancer Res 2007;67:5976–82.
31. Kumar AP, Bhaskaran S, Ganapathy M, et al. Akt/cAMP-responsive element binding protein/cyclin D1 network: a novel target for prostate cancer inhibition in transgenic adenocarcinoma of mouse prostate model mediated by Nexrutine, a Phellodendron amurense bark extract. Clin Cancer Res 2007;13:2784–94.
32. Singh SV, Powolny AA, Stan SD, et al. Garlic constituent diallyl trisulfide prevents development of poorly-differentiated prostate cancer and pulmonary metastasis multiplicity in TRAMP mice. Cancer Res 2008;68:9503–11.
33. Chuang LC, Yew PR. Proliferating cell nuclear antigen recruits cyclin-dependent kinase inhibitor Xic1 to DNA and couples its proteolysis to DNA polymerase switching. J Biol Chem 2005;280:35299–309.
34. Jackson SJT, Singletary KW, Venema RC. Sulforaphane suppresses angiogenesis and disrupts endothelial mitotic progression and microtubule polymerization. Vascul Pharmacol 2006;46:77–84.
35. Wheelock MJ, Johnson KR. Cadherins as modulators of cellular phenotype. Annu Rev Cell Dev Biol 2003;19: 207–35.
36. Terabe M, Berzofsky JA. NKT cells in immunoregulation of tumor immunity: a new immunoregulatory axis. Trends Immunol 2007;28:491–6.
37. Guerra N, Tan YX, Joncker NT, et al. NKG2D-Deficient mice are defective in tumor surveillance in models of spontaneous malignancy. Immunity 2008;28:571–80.
38. Fernandez NC, Lozier A, Flament C, et al. Dendritic cells directly trigger NK cell functions: cross-talk relevant in innate anti-tumor immune responses *in vivo*. Nat Med 1999;5:405–11.
39. Hu R, Hebbar V, Kim BR, et al. *In vivo* pharmacokinetics and regulation of gene expression profiles by isothiocyanate sulforaphane in the rat. J Pharmacol Exp Ther 2004;310:263–71.
40. Hanlon N, Coldham N, Gielbert A, et al. Absolute bioavailability and dose-dependent pharmacokinetic behavior of dietary doses of the chemopreventive isothiocyanate sulforaphane in rat. Br J Nutr 2008;99:559–64.
41. Al Janobi AA, Mithen RF, Gasper AV, et al. Quantitative measurement of sulforaphane, iberin and their mercapturic acid pathway metabolites in human plasma and urine using liquid chromatography-tandem electrospray ionization mass spectrometry. J Chromatogr B 2006;844:223–34.
42. Cornblatt BS, Ye L, Dinkova-Kostova AT, et al. Preclinical and clinical evaluation of sulforaphane for chemoprevention in the breast. Carcinogenesis 2007;28: 1485–90.
43. Nelson WG, DeMarzo A, Isaacs WB. Prostate cancer. N Engl J Med 2003;349:366–81.
44. Fidler IJ, Kim SJ, Langley RR. The role of the organ microenvironment in the biology and therapy of cancer metastasis. J Cell Biochem 2007;101:927–36.
45. Nouri-Shirazi M, Banchereau J, Bell D, et al. Dendritic cells capture killed tumor cells and present their antigens to elicit tumor-specific immune responses. J Immunol 2000;165:3797–803.
46. Karimi K, Boudreau JE, Fraser K, et al. Enhanced antitumor immunity elicited by dendritic cell vaccines is a result of their ability to engage both CTL and IFNγ-producing NK cells. Mol Ther 2008;16:411–8.